JOURNAL OF SOLID STATE CHEMISTRY 108, 73–79 (1994)

The Synthesis and Structural Characterization of Na_3WO_3N

S. H. Elder,*,[1] F. J. DiSalvo,*,[2] J. B. Parise,† J. A. Hriljac,‡ and James W. Richardson, Jr.§

*Department of Chemistry, Baker Laboratory, Cornell University, Ithaca, New York 14853-1301; †Mineral Physics Institute, State University of New York at Stony Brook, Stony Brook, New York 11794; ‡Department of Physics, Brookhaven National Laboratory, Upton, New York 11973; §Intense Pulsed Neutron Source, Argonne National Laboratory, Argonne, Illinois 60439

Received February 16, 1993; accepted May 4, 1993

We report the discovery of a new ternary oxynitride, Na_3WO_3N. Na_3WO_3N is synthesized by exposing a eutectic melt consisting of $\frac{1}{2}Na_2O:1Na_2WO_4$ to a flow of ammonia gas at 695°C. The compound crystallizes in the acentric space group $Pmn2_1$ with a = 7.2481(3) Å, b = 6.2728(3) Å, and c = 5.6493(2) Å. The structure was determined from synchrotron X-ray powder diffraction data and refined using the Rietveld analysis on neutron powder diffraction data. It is isostructural to the low temperature form of Li_3PO_4 which can be derived from an ordered wurtzite structure-type with all the atoms having tetrahedral coordination. Alternatively, the structure can be described as being "salt-like" consisting of isolated $(WO_3N)^{-3}$ tetrahedral polyanions separated by Na^+.

INTRODUCTION

There have been a number of reports in the literature on the preparation of ternary nitrides and oxynitrides from ternary oxides and ammonia gas (1–3). These new materials have been studied to determine the presence of order/disorder in the anionic sites (4), to understand their dielectric properties (5), and to compare the electrical properties of reduced oxynitrides to reduced oxides (6). We discovered that $LiMoN_2$ could be synthesized by reacting Li_2MoO_4 in a flow of ammonia gas at 705°C (7). This prompted us to continue our search for new ternary nitrides that could be prepared using this general method, as well as to consider the thermodynamic arguments concerning these reactions (8). As part of this search, we have discovered a new oxynitride, Na_3WO_3N. Herein, we report the synthesis and structural characterization of this new compound.

EXPERIMENTAL

Synthesis

The title compound was first synthesized by heating approximately 0.5 g of $Na_2WO_4 \cdot 2H_2O$ (analytical reagent grade) in an alumina boat from room temperature to 700°C and holding at this temperature for 12 hr in a flow of ammonia gas (9). The reactant melted and a flocculent, black powder covered both the inside and outside of the boat. When viewed through a light microscope (150×), the powder was observed to be inhomogeneous, consisting of yellow and black particles. This mixed phase powder was ground in a mortar and pestle (all manipulations were carried out in an argon-filled glove box due to anticipated air sensitivity) and X-ray powder diffraction showed it to contain two crystalline phases. One phase was poorly crystallized and could be indexed as W_2N, but the other well crystallized phase could not be indexed as any known binary or ternary oxide, nitride (including the previously discovered Na_3WN_3 (10)), or oxynitride. When the mixed phase powder was put into water, the yellow fraction reacted vigorously with the production of ammonia gas, but the black phase appeared to be unaffected by water. The black phase was filtered from the aqueous slurry, washed, dried, and was determined to be unreacted W_2N by X-ray powder diffraction. The mass of the isolated W_2N was ~40% of the two-phase ammonolysis product which suggested that a reaction similar to the following had occurred:

$$3Na_2WO_4 \cdot 2H_2O + \tfrac{38}{3}NH_3 \rightarrow 2Na_3WN_3 + \tfrac{1}{2}W_2N + \tfrac{7}{6}N_2 + 14H_2O \quad [1]$$

We suspected a new ternary nitride had formed, possibly a new structural form of Na_3WN_3. However, we could not rule out the possibility that we were synthesizing a new, moisture-sensitive oxynitride.

When $Na_2WO_4 \cdot 2H_2O$ (which loses $2H_2O$ at 100°C in air) was heated in an ammonia flow to temperatures less than ~650°C for 12 hr, only a small fraction of the new phase was seen in the X-ray powder diffraction pattern of the resulting product; the two major polycrystalline phases observed in the pattern were unreacted Na_2WO_4 and W_2N. When $Na_2WO_4 \cdot 2H_2O$ was heated (Na_2WO_4 melts at 696°C) in air and then exposed to a flow of ammo-

[1] Current Address: Laboratoire de Chimie des Solides, Institut des Matériaux de Nantes, 2 Rue de la Houssiniere, 44072 Nantes, France.
[2] To whom correspondence should be addressed.

0022-4596/94 $6.00

nia gas, a reaction was observed to occur after about 10 min. The reaction melt began bubbling with the formation of a small amount of black solid. The liquid remained clear and colorless. If this reaction was terminated after 20 min by fast cooling (~30 min), W_2N and Na_2WO_4 were once again the only polycrystalline phases observed in the X-ray powder diffraction pattern. However, when the heating was continued for 10–12 hr at 700°C, only W_2N and the new phase existed. At temperatures between 725 and 925°C, the new phase was entirely decomposed leaving only W_2N and W metal and at 960°C only W metal could be observed by X-ray powder diffraction.

We suspected that the new phase had a greater Na : W ratio than the initial Na_2WO_4 stoichiometry, as the reaction in Eq. [1] indicates. To compensate for the loss of tungsten as W_2N, a reaction mixture of $\frac{1}{2}Na_2O_2$ and 1 Na_2WO_4 was used. The two powders were ground together in a glove box and the loose powder was heated in an alumina boat, in air, to 560°C in 6 hr. Na_2O_2 loses $\frac{1}{2}O_2$ at red heat resulting in the formation of Na_2O (11). The temperature was rapidly (~10 min) increased above the eutectic temperature of 600 to 695°C. The melt was next exposed to a flow of ammonia gas as before and was reacted under these conditions for 12 hr. We found that the melt slowly crawled up the sides of the alumina boat, and if it was not reacted with ammonia, the melt would "spill out" and attack the quartz flow tube. This was minimized by the rapid heating from 560 to 695°C.

The reaction product was a bright yellow solid with only a small amount (<5% by mass) of black powder at the fringes of the once eutectic melt. There was a distinct boundary between the pure yellow solid and the yellow/black, mixed-phase solid at the perimeter of the reaction mass, hence the black solid was easily scraped away. X-ray powder diffraction indicated that the yellow solid was the pure, new phase seen before, while the black solid was W_2N, also seen previously. By eye it appeared that the yellow/black portion of the product was at least 75% yellow phase which was verified by mass loss when this portion was reacted with water, filtered, washed, and dried. We now exclusively synthesize the new phase by this method.

The production of a small amount of W_2N, even when the Na : W ratio was 3 : 1 in the initial reaction mixture, suggests that some volatile phase is being formed and continuously swept away by the ammonia flow and/or the yellow phase is not thermodynamically stable under the reaction conditions used. When the *pure* yellow phase was re-reacted in ammonia gas at 695°C, black W_2N was observed to form within an hour. We have previously observed a similar decomposition process in $LiMoN_2$ when it is made from the ternary oxide, Li_2MoO_4, at 705°C.

Analysis

Solutions of the yellow phase were prepared by dissolution of the solid in slightly basic (0.02% NH_3 by volume) distilled water. Basic conditions were necessary to keep the tungsten species from precipitating out of solution. Standard tungsten and sodium solutions were prepared by diluting tungsten and sodium ICP/DCP standard solutions (Aldrich Chemical Co.) with distilled water and concentrated ammonium hydroxide solution (again, 0.02% by volume), as before. Metals analysis on these solutions were carried out using plasma emission spectroscopy (PES). The tungsten line (λ = 180.7 nm) and the sodium line (λ = 589.6 nm) were analyzed on a Jarrel-Ash I.C.A.P. 61 update spectrometer. The Na : W ratio was found to be 3.07 : 1 (expected accuracy of ±2%). We inferred from the yellow color of the new phase that the tungsten was fully oxidized (d^0) hence, we expected a stoichiometry of Na_3WN_3 (a new structural form) or Na_3WO_3N.

Using the modified Dumas method (12), we attempted to analyze the nitrogen content of the yellow phase. The yellow phase appeared to react completely in CO_2 at 1000°C (the sample melted and was white as expected for a $\frac{1}{2}Na_2O$: $1Na_2WO_4$ mixture), but only 19% of the theoretical amount of nitrogen was collected if the starting solid was assumed to be Na_3WN_3. At this point it was clear that this new material was not a "pure" nitride, but a new oxynitride. We then sought a more accurate means of measuring the nitrogen content.

We employed a spectrophotometric method for the determination of ammonia that was produced when the pure yellow phase was dissolved in a weakly acidic solution (13). Gelatin capsules were filled with approximately 140 mg samples of the yellow phase. These capsules were brought out of the dry box and dropped into 500 ml volumetric flasks that were ~$\frac{1}{2}$ full with a 0.10% (by volume) sulfuric acid solution. The flasks were immediately capped and inverted. The capsule dissolved in about 10 min exposing the sample to the solution which subsequently produced ammonium sulfate. The flasks were shaken for several hours to *attempt* to quantitatively "trap" all the evolved ammonia as ammonium sulfate. A blank gelatin capsule was also treated in a similar manner to determine what contributions, if any, it would make to the analysis. All flasks were diluted to 500 ml with distilled water to make stock solutions. A 0.15-ml aliquot from a stock solution was added to 2.0 mL of a solution that contained 8.5% sodium salicylate and 0.03% sodium nitroprusside. The color development was initiated by adding to this mixture 2.0 ml of a solution that contained 1.5 g/liter sodium dichloroisocyanurate and 12 g/liter sodium hydroxide. The absorbance of this solution was measured on a Milton Roy 1001Plus spectrophotometer and its optical density was converted to an ammonia concen-

tration by means of a standard curve prepared by applying this method to a series of ammonium sulfate standards. We then converted the ammonium concentration to nitrogen content in the original yellow phase.

An average of 91.9% of the theoretical amount of nitrogen was measured if we assumed a sample stoichiometry of Na_3WO_3N. This analytical method typically has an accuracy of ±1% in studies on standard samples (nitrogen containing biological specimens) obtained from the National Institute of Standards and Technology (NIST) (14). The difficulty in quantitatively "trapping" all the ammonia as ammonium with the technique used may have lead to our results of finding less nitrogen than we expected. Considering this argument we will refer to this phase as Na_3WO_3N which would result from the following reaction:

$$\tfrac{1}{2}Na_2O : 1Na_2WO_4 + NH_3 \rightarrow Na_3WO_3N + \tfrac{3}{2}H_2O \quad [2]$$

The measured density (15) for Na_3WO_3N of 4.00 g cm^{-3} (±2%) compared well with the theoretical density of 4.07 g cm^{-3} for $Z = 2$ (see section on structure determination and refinement).

STRUCTURE DETERMINATION AND REFINEMENT

X-Ray Diffraction

Initial X-ray powder diffraction data were collected with a Scintag XDS 2000 diffractometer using Cu$K\alpha$ radiation. We chose 27 of these reflections, that were well resolved, as input data for TREOR (16) to determine the unit cell and the lattice type for Na_3WO_3N. All 27 reflections were indexed on a hexagonal unit cell with a = 14.481 Å and c = 5.643 Å (figure of merit, M_{20} = 28) (17). Realizing that there were a large number of systematic zeroes with the hexagonal indexing, we limited the maximum unit cell volume to 500 Å^3. Again, the indexing program TREOR was employed and the same 27 reflections were indexed on an orthorhombic unit cell with a = 7.251 Å, b = 6.273 Å, and c = 5.647 Å (figure of merit, M_{20} = 37). The orthorhombic unit cell volume (256.8 Å^3) is exactly four times smaller than the hexagonal cell (1024.8 Å^3). Since the hexagonal indexing produced a large number of systematic zeroes, many more than expected from a hexagonal space group, it seemed likely that the true cell symmetry was orthorhombic. Table 1 lists the calculated and observed d-spacings and the calculated relative intensities for the reflections allowed for Na_3WO_3N (18). There was a slight discrepancy in intensity between the calculated and experimental data at low angle due to the small sample holder used.

Considering that there were many closely overlapping reflections in the preliminary X-ray data, we collected synchrotron X-ray powder diffraction data to obtain as many well resolved reflections as possible to determine the likely space group(s) for Na_3WO_3N. The sample was loaded into a thin-walled (0.5 mm I.D.) quartz capillary and measurements were performed at the X7A beam line at the National Synchrotron Light Source (NSLS), Brookhaven National Laboratory (19). The wavelength used for the experiments (1.2279 Å) was chosen with a Ge (111) channel-cut monochromator and the exact value was determined by calibration with a reference sample of CeO_2.

TABLE 1
Calculated and Observed d Spacings and Calculated Relative Intensities for Na_3WO_3N from X-ray Powder Diffraction (Cu$K\alpha$ Radiation)

$h\ k\ l$	d_{obs}(Å)	d_{calc}(Å)	I_{calc}(%)
0 1 0	6.267	6.272	27.0
1 1 0	4.739	4.743	88.7
1 0 1	4.451	4.453	100
0 1 1	4.193	4.198	64.2
1 1 1[a]		3.632	25.9
2 0 0	3.626	3.624	26.4
2 1 0	3.134	3.138	38.9
0 2 0[a]		3.136	21.4
1 2 0	2.876	2.878	17.0
0 0 2	2.822	2.825	42.8
2 1 1	2.741	2.743	76.8
0 2 1[a]		2.742	35.9
0 1 2[a]		2.575	4.50
1 2 1	2.562	2.564	12.0
1 1 2	2.425	2.427	23.3
2 2 0	2.371	2.371	2.90
3 1 0	2.255	2.254	9.32
2 0 2	2.225	2.228	11.8
3 0 1[a]		2.221	11.6
2 2 1	2.185	2.186	19.1
2 1 2	2.099	2.099	17.5
0 2 2[a]		2.0987	9.45
3 1 1[a]		2.094	7.81
0 3 0	2.089	2.091	5.19
1 2 2	2.015	2.016	12.4
1 3 0	2.008	2.009	0.59
0 3 1[a]		1.961	0.33
3 2 0	1.913	1.914	7.12
1 3 1	1.892	1.893	15.8
1 0 3	1.820	1.823	8.91
2 2 2[a]		1.816	3.28
3 2 1		1.813	3.01
4 0 0[a]		1.812	14.8
2 3 0[a]		1.811	28.8
0 1 3[a]		1.804	6.51
3 1 2	1.761	1.762	9.43

Note. (Observed intensities are not reported because of the slight discrepancy between the calculated and observed data at low angle due to the small sample holder used.)

[a] Refers to observed reflections that could not be indexed due to other closely overlapping reflections.

A Kevex detector, a 0.4-mm receiving slit and an incident beam-defining slit of 8.0 mm by 0.8 mm, define the remainder of the diffraction conditions. The X-ray data were collected in three scans, from 5 to 25°, from 25 to 45°, and from 45 to 70° in 2θ with a step size of 0.01° and counting times of 4, 8, and 12 sec, respectively.

Based on the orthorhombic indexing and the systematic absences observed in the synchrotron X-ray data of: $(00l)$, $l = 2n + 1$; $(h00)$, $h = 2n + 1$ and $(h0l)$, $h + l = 2n + 1$, we could limit the possible space groups to $Pmn2_1$ (No. 31) and $Pmnm$ (No. 59). We then searched the structural literature (20) for compounds that exhibit structures in one of these space groups with three different atoms in a 3 : 1 : 4 stoichiometry (assuming that the three oxygens and one nitrogen are disordered). We found only one example, the low temperature form of Li_3PO_4which crystallizes in the acentric space group $Pmn2_1$ (21).

Neutron Diffraction

Locating the nitrogen and oxygen positions (and possibly the sodium positions) in the presence of tungsten may be more facile with neutron powder diffraction rather than X-ray powder diffraction data due to the small X-ray scattering factors of these atoms compared to that of tungsten. Time-of-flight neutron diffraction data were collected on a 5.5-g sample of Na_3WO_3N loosely packed into a 5/8″ diameter vanadium can in an argon-filled dry box. A cap was sealed to the top of this can with indium metal to prevent air exposure. The experiments were carried out on the General Purpose Powder Diffractometer (GPPD) at the Intense Pulsed Neutron Source (IPNS), Argonne National Laboratory. Measurements were made for about 10 hr at 298 and 15 K with detector banks at 60°, 90°, and 148° in 2θ.

The atomic positions for Li_3PO_4, along with the lattice constants calculated by TREOR (orthorhombic indexing) for Na_3WO_3N, were used as a starting model for the Rietveld refinement of the Na_3WO_3N neutron powder diffraction data (22). The neutron powder pattern is shown in Fig. 1. We chose to refine the data from the high resolution, 148° bank. Table 2 lists the positional and thermal parameters for the room temperature refinement. Table 3 lists pertinent bond distances and angles. In this refinement the 6 oxygens and 2 nitrogens (per unit cell) were disordered over the three anionic crystallographic sites and the nitrogens/oxygens in each individual site were constrained to have equal x, y, z, and U_{iso} parameters. Also, the sum of the occupation factors for each individual anionic site were constrained to be one and the z parameter of the tungsten was fixed at zero in order to define the origin along the c axis.

Three other refinements were carried out on the room temperature data in which the nitrogen was ordered on each of the three crystallographic distinct anionic sites. Only in the case where the nitrogen was preferentially ordered on the 4*b* site did the refinement converge; however, the fit to the data was not improved over the disordered model.

Analogous refinements were performed on low temperature data (15 K). The disordered and ordered (nitrogen on the 4*b* site) refinements converged smoothly with structural characteristics very similar to the room temperature refinements.

DISCUSSION

It is interesting to compare the similarities between the reaction conditions and thermal stability of Na_3WO_3N and $LiMoN_2$. The synthesis temperature of both compounds is optimal at the melting point of the respective ternary oxide, Na_2WO_4 and Li_2MoO_4 (mp = 705°C). If the reaction temperature is 650°C or less for either reaction, the kinetics of the reaction are slow enough that essentially no oxynitride or ternary nitride is formed. At temperatures greater than ~30°C above the optimal reaction temperature, neither the oxynitride or the ternary nitride is stable. We are currently investigating the thermochemistry of both of these compounds to gain an understanding of why an oxynitride is formed from Na_2WO_4 while the ternary nitride is formed from Li_2MoO_4 (8). Na_3MoO_3N can also be prepared from Na_2MoO_4 under similar reaction conditions. It is isostructural to Na_3WO_3N.

The structure of Na_3WO_3N is based on an ordered wurtzite superlattice (Fig. 2). This structure type is well known and has been studied in great detail (24). In contrast, the structure of Ba_3WN_4 (25) can be derived from the Na_3As structure-type. With this view of the structure, it is obvious why the X-ray powder diffraction pattern could be alternatively indexed on a larger hexagonal cell. One distorted hexagonal sub-lattice is formed by 3Na/1W in an ordered arrangement and these metal polyhedra are centered by 3O/1N. Hence, the anions also form a distorted hexagonal sublattice. All the cations and anions are in tetrahedral coordination. The W–N/O distances of 1.81 and 1.77 Å and the Na–N/O distances of 2.3–2.4 Å (Table 2) are comparable to the W–O (tetrahedrally coordinated tungsten) and Na–O (octahedrally coordinated sodium) distances found in $Na_2W_2O_7$ (1.80–2.06 and 2.4–2.6 Å, respectively) (26) and the W–N and Na–N distances in Na_3WN_3 (1.78–1.93 and 2.32–2.99 Å, respectively).

Alternatively, this structure can be described as being "salt-like" (Fig. 3). It consists of isolated $(WO_3N)^{-3}$ tetrahedra separated by Na^+, also in tetrahedral coordination. These structure-types are favorable when excess electropositive metal is present and there have been many new ternary nitrides reported that belong to this general structure class (27, 28).

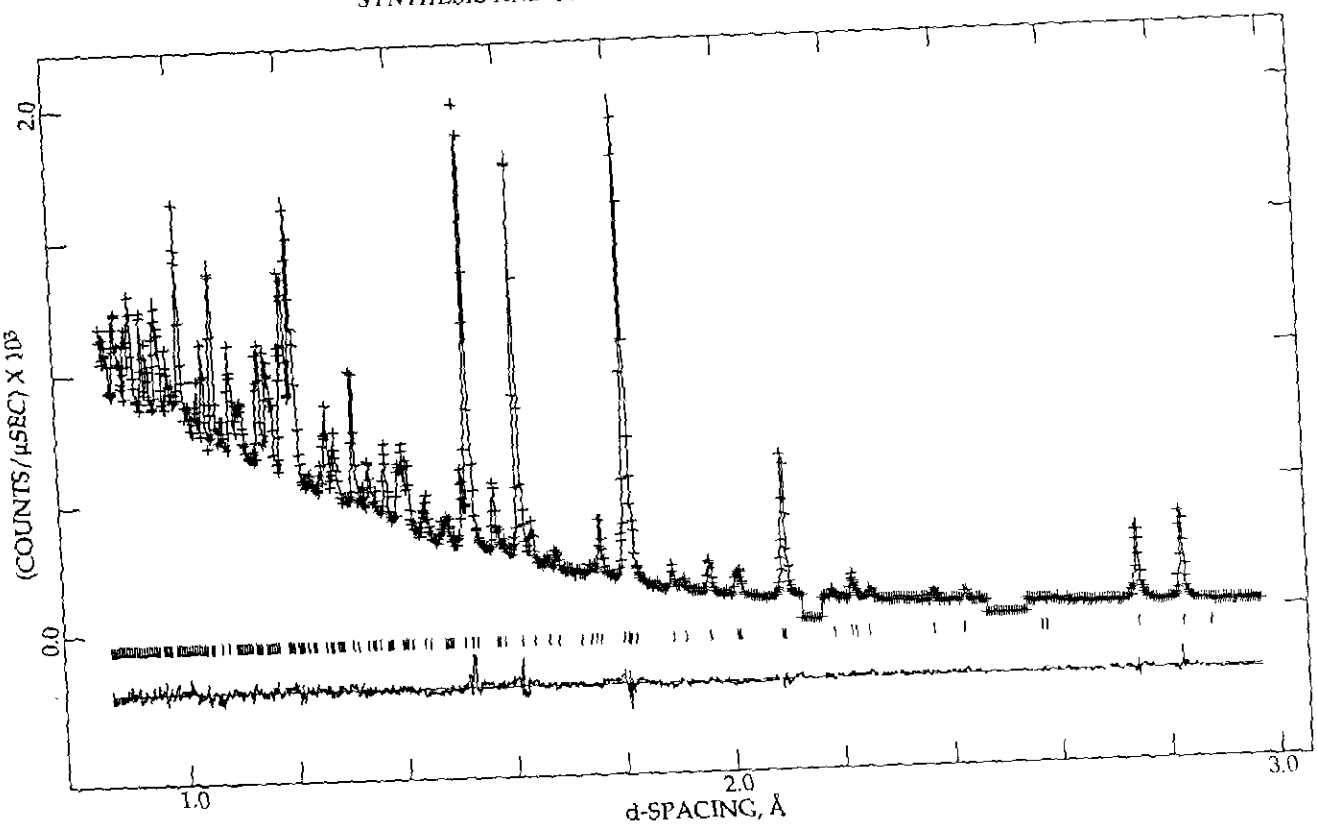

FIG. 1. Time-of-flight neutron diffraction data (*t48° bank*) for Na_3WO_3N collected at 298 K at the Intense Pulsed Neutron Source (IPNS) at Argonne National Laboratory. Points shown by + represent observed data. The continuous line through the sets of points are the calculated profiles from the refinement given in Table 1. The tick marks below the data indicate the positions of the allowed reflections for Na_3WO_3N and the lower curve represents the difference between observed and calculated profiles. Gaps in the pattern are regions containing peaks arising from impurities (the intensity of these impurity peaks were much less than 1% of the most intense peak for Na_3WO_3N) and were excluded from the refinement.

It is reasonable to consider the nitrogen to be ordered on the W–O/N(2) 2*a* site since this bond distance is the shortest of the three different tungsten–anion bonds. Bond valence calculations (*29*, *30*) showed this site to have the largest v_{ij} value (1.66 ± 0.04) for the disordered and ordered room temperature models. The bond valence sum (V_{ij}) in each case was 6.12 ± 0.13 and 6.05 ± 0.17, respectively. However, the refine-

TABLE 2
Refined Positional and Thermal Parameters from the Room Temperature Neutron Diffraction Data Refinement of Na_3WO_3N (N and O Disordered), $Z = 2$

Atom	Site	*x*	*y*	*z*	U_{iso} (Å² × 100)
W	2*a*	0.0	0.8280(10)	0.0	2.2(1)
Na(1)	2*a*	0.5	0.8420(10)	0.9800(8)	3.5(2)
Na(2)	4*b*	0.2456(4)	0.3326(7)	0.9758(7)	2.9(1)
O/N(1)[a]	2*a*	0.0	0.1021(3)	0.8960(7)	3.2(1)
O/N(2)[a]	2*a*	0.5	0.1752(6)	0.8139(6)	3.6(1)
O/N(3)[a]	4*b*	0.2054(2)	0.6919(2)	0.8988(5)	2.2(1)

Note. $a = 7.2481(3)$, $b = 6.2728(3)$, $c = 5.6493(2)$ Å, $R_N = 4.44\%$, $R_p = 2.86\%$, $R_{wp} = 2.94\%$ and $X^2 = 1.30$ for 336 reflections. The final refinement involved 13 atom coordinates, 6 isotropic temperature factors, 3 lattice parameters, 1 scale factor, 1 absorption coefficient, 1 zero point parameter, 8 profile coefficients (23) and 6 background parameters (cosine Fourier series).

[a] The occupancy of this site is 0.75O/0.25N.

TABLE 3
Selected Interatomic Distances (Å) and Angles (deg) from the Room Temperature Refinement of Na_3WO_3N (O and N Disordered)

	Bond distances		
W(1)–O/N(1)	1.811(7)	Na(1)–O/N(3) × 2	2.380(5)
W(1)–O/N(2)	1.768(4)	Na(2)–O/N(1)	2.338(5)
W(1)–O/N(3) × 2	1.812(4)	Na(2)–O/N(2)	2.283(5)
Na(1)–O/N(1)	2.363(5)	Na(2)–O/N(3)	2.319(8), 2.414(4)
Na(1)–O/N(2)	2.297(10)		
	Angles		
O/N(1)–W(1)–O/N(3) × 2	110.16(17)	O/N(2)–Na(1)–O/N(3)	104.70(21)
O/N(1)–W(1)–O/N(2)	109.9(4)	O/N(3)–Na(1)–O/N(3)	105.50(26)
O/N(2)–W(1)–O/N(3) × 2	108.11(19)	O/N(1)–Na(2)–O/N(2)	105.9(4)
O/N(3)–W(1)–O/N(3)	110.37(32)	O/N(1)–Na(2)–O/N(3) × 2	104.76(14)
O/N(1)–Na(1)–O/N(3)	117.80(20)	O/N(2)–Na(2)–O/N(3) × 2	106.05(18)
O/N(2)–Na(1)–O/N(3)	116.47(21)	O/N(3)–Na(2)–O/N(3)	127.7(4)
O/N(1)–Na(1)–O/N(2)	105.62(29)		
O/N(1)–Na(1)–O/N(3)	105.48(22)		

ments diverged when the nitrogen was ordered on this 2*a* site.

Both room- and low-temperature neutron diffraction data were collected in hopes that we could determine whether the nitrogen and oxygen order crystallographically. Since the scattering lengths of oxygen (0.580×10^{-12} cm) and nitrogen (0.94×10^{-12} cm) are quite different, we expected to detect any ordering. The residuals from the room temperature and low temperature refinements were not statistically improved by assuming nitrogen to preferentially occupy any one of the anionic sites and it would appear that oxygen and nitrogen are completely disordered over the anion sites as has been seen in other oxynitride systems (4).

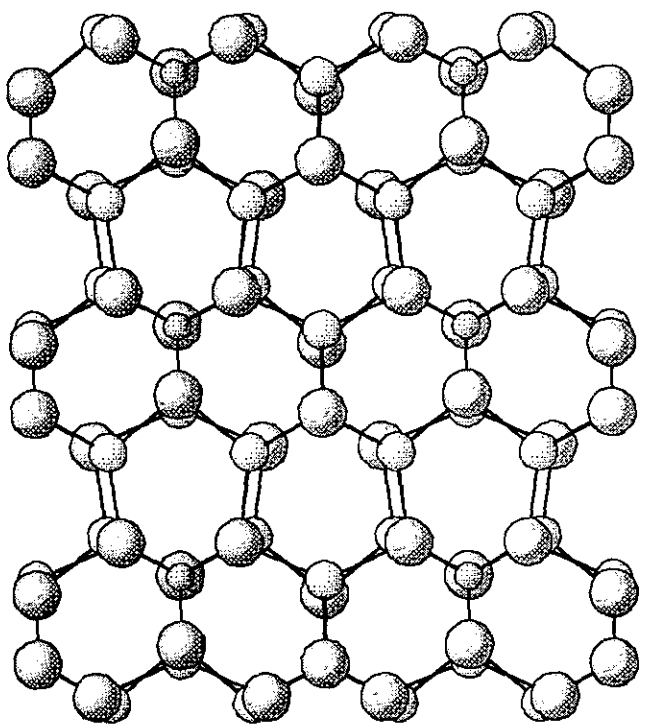

FIG. 2. A view of a portion of the Na_3WO_3N structure emphasizing the distorted hexagonal-lattice network (in the (001) direction). The small circles represent W, the medium circles Na, and the large circles 0.75O/0.25N sites.

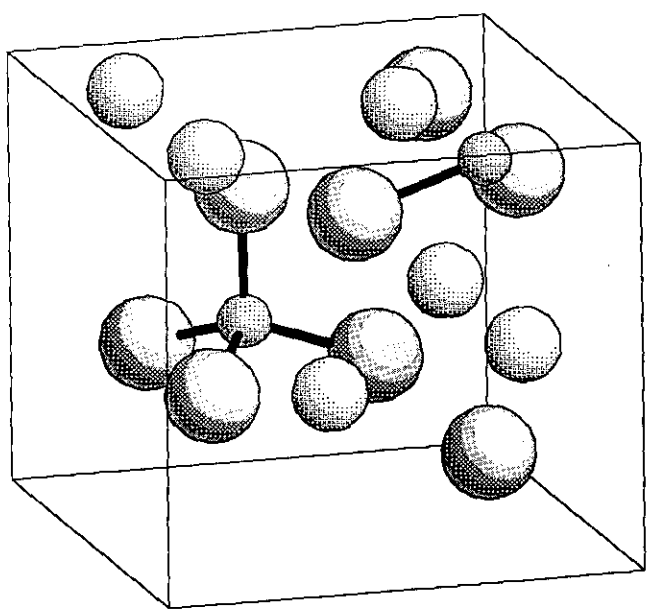

FIG. 3. The unit cell for Na_3WO_3N emphasizing the $(WO_3N)^{-3}$ tetrahedral polyanions. The small circles represent W, the medium circles Na, and the large circles 0.75O/0.25N sites.

ACKNOWLEDGMENTS

We are grateful to the Office of Naval Research for its generous support of our nitride work. We are also grateful to Mike Rutzke in the Department of Fruit and Vegetable Sciences at Cornell University for assistance in the PES and nitrogen analysis.

This work has benefited from the use of the Intense Pulsed Neutron Source at Argonne National Laboratory which is funded by the U.S. Department of Energy, BES-Materials Science, under Contract W-31-109-Eng-38 and from the use of the National Synchrotron Light Source at Brookhaven National Laboratory which is funded by the U.S. Department of Energy, BES-Materials Science Contract DE-AC02-76CH00016 and Division of Materials Sciences and Chemical Sciences.

J.B.P. acknowledges the generous support by the National Science Foundation for his research through Grant DMR 90-24249.

REFERENCES

1. G. Liu, X. Zhao, and H. A. Eick, *J. Alloys Comp.* **187,** 145 (1992).
2. F. Pors, R. Marchand, and Y. Laurent, *Ann. Chim. Fr.* **16,** 547 (1991).
3. R. Marchand, F. Pors and Y. Laurent *Ann. Chim. Fr.* **16,** 553 (1991).
4. P. Bacher, P. Antoine, R. Marchand, P. L'Haridon, Y. Laurent, and G. Roult, *J. Solid State Chem.* **77,** 67 (1988).
5. R. Marchand, F. Pors, Y. Laurent, O. Regreny, J. Lostec, and L. M. Haussonne, *J. Phys. Colloq.* **47**(2), C1-901 (1986).
6. P. Antoine, R. Marchand, Y. Laurent, C. Michel, and B. Raveau, *Mat. Res. Bull.* **23,** 953 (1988).
7. S. H. Elder, L. H. Doerrer, F. J. DiSalvo, J. B. Parise, D. Guyomard, and J. M. Tarascon, *Chem. Mater.* **4,** 928 (1992).
8. S. H. Elder, F. J. DiSalvo, and A. Navrotsky, to be published.
9. P. E. Rauch and F. J. DiSalvo, *Inorg. Synth.*, in press.
10. D. Ostermann, U. Zachwieja, and H. Jacobs, *J. Alloys Comp.* **190,** 137 (1992).
11. G. Brauer, "*Handbook of Preparative Inorganic Chemistry,*" p. 979. Academic Press, New York, 1963.
12. D. G. Czechowicz, Los Alamos National Laboratory, personal communication, 1989.
13. R. L. Searcy, J. E. Reardon, and J. A. Foreman, *Am. J. Med. Technol.* **33**(1), 15 (1967).
14. M. Rutzke, Cornell University, personal communication, 1993.
15. M. Y. Chern, R. D. Mariani, D. A. Vennos, and F. J. DiSalvo, *Rev. Sci. Instrum.* **61,** 1733 (1990).
16. P.-E. Werner, L. Eriksson, and M. Westdahl, *J. Appl. Crystallogr.* **18,** 367 (1985).
17. P. M. DeWolff, *J. Appl. Crystallogr.* **1,** 108 (1968).
18. K. Yvon, W. Jeitschko, and E. Parthe, *J. Appl. Crystallogr.* **10,** 73 (1977).
19. D. E. Cox, B. H. Toby, and M. M. Eddy, *Aust. J. Phys.* **41,** 117 (1988).
20. Joint Committee on Powder Diffraction Standards (JCPDS) on-line search.
21. C. Keefer, A. Mighell, F. Mauer, H. Swanson, and S. Block, *Inorg. Chem.* **6**(1), 119 (1967).
22. A. C. Larson, and R. B. Von Dreele, "Generalized Structural Analysis System." LANCE, MS-H805, Los Alamos National Laboratory, Los Alamos, NM 87545.
23. R. B. Von Dreele, J. D. Jorgensen, and C. G. Windsor, *J. Appl. Cryst.* **15,** 581 (1982), modified by R. B. VonDreele, unpublished (1983).
24. M. O'Keeffe and B. G. Hyde, *Acta Crystallogr. Sect. B* **34,** 3519 (1978).
25. A. Gudat, P. Hohn, R. Kniep, and A. Rabenau, *Z. Naturforsch. B*, in press.
26. I. Lindqvist, *Acta Chem. Scand.* **4,** 1066 (1950).
27. D. A. Vennos, M. E. Badding, and F. J. DiSalvo, *Inorg. Chem.* **29,** 4059 (1990).
28. P. Hohn, R. Kniep, and A. Rabenau, *Z. Kristallog.*, in press.
29. I. D. Brown and D. Altermatt, *Acta. Crystallogr. Sect. B* **41,** 244 (1985).
30. N. E. Brese and Michael O'Keeffe, *in* "Structure and Bonding" (M. J. Clarke *et al.*, Eds.), p. 307. Springer-Verlag, Berlin, 1992.